agronomy

MDPI

Article

Genome-Wide Identification of the Maize *ZmGeBP* Gene Family and Functional Characterization of *ZmGeBP8* in Stress Tolerance

Jiaxin Wang [1,2,†], Meiling Wang [1,2,†], Yang Liu [1,2], Qiuyu Ma [1,2], Yongfeng Song [1,2], Hexuan Liu [1,2], Yuyang Zhou [1,2], Yu Zhou [1,2], Lin Zhang [1,2], Xing Zeng [1,2], Zhenhua Wang [1,2], Chunxiang Li [1,2,*] and Hong Di [1,2,*]

[1] Northeast Agricultural University, Harbin 150030, China; 15103869531@163.com (J.W.); 18345488794@163.com (M.W.); 16629070073@163.com (Y.L.); 15046541060@163.com (Q.M.); song18182746326@163.com (Y.S.); liuhexuan11121@163.com (H.L.); zyyneau@163.com (Y.Z.); zhouyu0924@126.com (Y.Z.); neauzla@163.com (L.Z.); zengxing@neau.edu.cn (X.Z.); zhenhuawang_2006@163.com (Z.W.)
[2] Key Laboratory of Germplasm Enhancement, Physiology and Ecology of Food Crops in Cold Region, Northeast Agricultural University, Ministry of Education, Harbin 150030, China
* Correspondence: lcx990127@163.com (C.L.); dihongdh@163.com (H.D.)
† These authors contributed equally to this work.

Abstract

GLABROUS1 enhancer-binding protein (GeBP) family members are plant-specific transcription factors involved in growth, development, and environmental responses. However, the characteristics and stress-responsive patterns of this family in maize (*Zea mays* L.), particularly during seed aging and saline–alkali stress, remain insufficiently understood. We identified 19 *ZmGeBP* genes and classified their encoded proteins into four phylogenetic groups together with homologs from sorghum and rice. Duplication and synteny analyses showed that segmental duplication was the predominant duplication pattern detected in maize and that collinear relationships were retained among the three grasses. The *ZmGeBP* promoters contained cis-acting elements associated with development, light, phytohormone responses, and stress. RT-qPCR analysis of seven selected genes revealed temporal and genotype-dependent expression patterns during artificial seed aging and saline–alkali stress. Subcellular localization confirmed nuclear targeting of *ZmGeBP8*, and dual-luciferase reporter assays showed that *ZmOCL13* reduced *ZmGeBP8* promoter activity, suggesting a potential repressive effect. Overall, these findings elucidate the molecular features of maize *ZmGeBP* genes and establish a framework for validating their roles in stress resilience.

Keywords: *Zea mays* L.; *ZmGeBP* gene family; genome-wide analysis; seed aging; saline–alkali stress

Check for updates

Academic Editor: Francesca Taranto

Received: 28 September 2026
Revised: 18 October 2026
Accepted: 22 October 2026
Published: 25 October 2026

Copyright: © 2026 by the authors. Licensee MDPI, Basel, Switzerland. This article is an open access article distributed under the terms and conditions of the Creative Commons Attribution (CC BY) license.

1. Introduction

As a global staple, maize (*Zea mays* L.) underpins human nutrition, animal feed, and industrial applications [1]. Nevertheless, environmental challenges routinely restrict maize yields, causing severe loss of seed vigor during aging and stress exposure [2]. Numerous studies have demonstrated that seed deterioration is regulated by complex interactions between endogenous genetic factors and environmental cues, including storage temperature, relative humidity, and oxygen partial pressure. Endogenous factors, including chlorophyll content, seed coat structure, phytohormone balance, reactive oxygen species levels, and nucleic acid and protein integrity and repair, are also involved in the control of seed

longevity [3]. Maize copes with unfavorable conditions through coordinated physiological, metabolic, and transcriptional reprogramming [4]. In these adaptive pathways, transcription factors serve as master switches that bind specific *cis*-acting elements within target promoters to modulate gene expression, thereby driving developmental shifts and stress resilience [5–7].

The GLABROUS1 ENHANCER-BINDING PROTEIN (*GeBP*) family represents a plant-specific group of transcription factors. GeBP proteins feature a conserved central DNA-binding domain (DUF573) of unknown precise molecular function, coupled with an atypical C-terminal leucine-zipper-like motif distinct from canonical bZIP structures [8]. Initially identified in *Arabidopsis thaliana* as a nuclear protein regulating epidermal cell differentiation via the *GLABROUS1* (*GL1*) enhancer [9], *GeBP* and its related proteins have since been implicated in hormone cross talk, organogenesis, and environmental stress responses. *Arabidopsis GeBP/GPL* members form homo- or heterodimers through their non-canonical leucine zippers to redundantly govern cytokinin signaling, with *GPL4* additionally mediating root avoidance under cadmium, copper, and zinc toxicity [10,11]. In *Brassica rapa*, *BrGeBP3*, *BrGeBP14*, and *BrGeBP17* respond to drought, whereas *BrGeBP5* acts downstream of *miR172* during cold adaptation [12]. Likewise, *Malus domestica MdGeBP3* coordinates adventitious rooting, flowering, cytokinin and abscisic acid sensitivity, and drought responses [13]. Seed aging induces oxidative damage, energy disruption, altered phytohormone profiles, and wide-scale transcriptional shifts that compromise seed viability, similar to the physiological shocks caused by saline–alkali conditions in maize [14–16]. Although several regulators of seed aging have been identified recently, the role of *ZmGeBP* genes in responding to seed deterioration or combined saline–alkali stress remains unexplored.

Genome-wide surveys have characterized *GeBP* genes in *Arabidopsis* [10], tomato [17], soybean [18], and common wheat [8]. Across gramineous crops, Huang et al. identified 125 *GeBP* genes across nine taxa, including 19 in maize [19]. However, their expression analyses focused primarily on rice, leaving the genetic and functional roles of maize *GeBP* genes under stress unvalidated. In this study, we comprehensively re-evaluated the *ZmGeBP* family to define their gene architecture, motif arrangements, promoter *cis*-elements, and stress-response expression patterns. Furthermore, we evaluated candidate *ZmGeBP* expression differences between two contrasting maize inbred lines under artificial seed aging and saline–alkali conditions. We selected *ZmGeBP8* for detailed functional analysis, verifying its nuclear localization and assessing its promoter regulation via transient reporter assays in *Nicotiana benthamiana*. This work establishes a foundation for decoding *ZmGeBP* function in maize seed longevity and abiotic stress tolerance.

2. Materials and Methods

2.1. Plant Materials and Stress Treatments

We utilized two maize (*Zea mays* L.) inbred lines bred by Northeast Agricultural University: the maize inbred line tolerant to both seed aging and saline–alkali stress Dong 156 and the stress-sensitive maize inbred line Dong 237 (Supplementary Figure S1). Two parallel experiments evaluated artificial seed aging and saline–alkali stress. For artificial aging, seeds were incubated at 45 °C and approximately 95% relative humidity for 4 d (96 h). For saline–alkali stress, surface-sterilized seeds were germinated on paper saturated with a salt mixture (5.0 mmol/L NaCl, 45.0 mmol/L Na_2SO_4, 45.0 mmol/L $NaHCO_3$, and 5.0 mmol/L Na_2CO_3). The final ion concentrations were 150.0 mmol/L Na^+, 45.0 mmol/L SO_4^{2-}, 45.0 mmol/L HCO_3^-, 5.0 mmol/L CO_3^{2-}, and 5.0 mmol/L Cl^-, with a solution pH of 9.7. Embryos were harvested at 0, 6, 14, 24, 30, and 40 h post-treatment. Each genotype, treatment, and time point included three biological replicates [16,20–22].

2.2. Identification of Maize GeBP Genes

Gene sequences, chromosomal locations, coding sequences (CDS), and protein profiles for *ZmGeBP* family members were retrieved from PlantTFDB (Table 1) [23]. Physicochemical properties were calculated using ExPASy ProtParam "https://web.expasy.org/protparam/ (accessed on 21 June 2026)" [24]. Open reading frame lengths, genomic positions, exon numbers, and strand orientation were obtained from Phytozome [25].

2.3. Phylogenetic Analysis

For phylogenetic classification, GeBP protein sequences from *Zea mays* L., *Sorghum bicolor*, and *Oryza sativa* were downloaded from Phytozome "https://phytozome-next.jgi.doe.gov/ (accessed on 21 June 2026)" (Supplementary Table S1) [25]. Sequences were aligned using the MUSCLE algorithm in MEGA 11 [26]. A neighbor-joining (NJ) tree was constructed in MEGA 11 using the Poisson substitution model with 1000 bootstrap replicates, then visualized and annotated in iTOL [27].

2.4. Analysis of Protein Conserved Motifs and Gene Structure of GeBP in Maize

Structural features of *ZmGeBP* genes were analyzed using TBtools (v2.476), while conserved motifs were identified using MEME "https://meme-suite.org/meme/ (accessed on 23 June 2026)" [28]. The XML motif output from MEME was imported into TBtools for visualization [29]. The amino acid sequences of the ZmGeBP proteins were submitted to AlphaFold Server "https://alphafoldserver.com/ (accessed on 23 June 2026)" for tertiary structure prediction [30]. The predicted structures were examined using the server's built-in visualization interface.

2.5. Analysis of Chromosomal Localization and Gene Collinearity

Chromosomal positions of *ZmGeBP* genes were mapped with TBtools using genomic coordinates [29]. Gene duplication events were identified via MCScanX in TBtools, and collinear relationships were displayed using the Circos module [29,31]. Scaffolds lacking assembly data were excluded. Interspecific synteny among maize, sorghum, and rice was visualized with the Dual Synteny Plot module in TBtools. To evaluate the selective pressures acting on duplicated *ZmGeBP* gene pairs, nonsynonymous substitution rates (Ka), synonymous substitution rates (Ks), and Ka/Ks ratios were calculated using TBtools. Ka/Ks ratios below, equal to, or above 1 were considered indicative of purifying, neutral, or positive selection, respectively [32]. The resulting Ka/Ks values were visualized using R.

2.6. Promoter Cis-Element Analysis

We extracted the 2000 bp upstream promoter sequences from the ATG start codon for each *ZmGeBP* gene via Phytozome. Stress- and hormone-responsive *cis*-regulatory elements were identified using PlantPAN [33] and mapped using the Basic Biosequence View module in TBtools-II.

2.7. Protein–Protein Interaction Network of ZmGeBP in Maize

Protein–protein interactions were predicted using STRING "https://string-db.org/ (accessed on 26 June 2026)" setting *Zea mays* as the target species [34]. The top 40 candidate interacting proteins ranked by confidence score were selected. Network construction and visualization were performed using the ggraph package (v2.1.0) in R (v4.3.1).

2.8. Expression Analysis Under Abiotic Stress, Saline–Alkali Stress, and Seed Aging

Public transcriptome datasets from MaizeGDB "https://maizegdb.org/ (accessed on 27 June 2026)" and NCBI "https://www.ncbi.nlm.nih.gov/ (accessed on 27 June 2026)" were analyzed to determine *ZmGeBP* expression in embryo and endosperm tis-

sues (PRJNA171684 and SRP010680) and under ultraviolet, salt, heat, and cold stresses (PRJNA244661) [25,35,36]. Expression trends were validated by reverse transcription quantitative PCR (RT-qPCR). Total RNA was isolated from embryos using TRIzol reagent, followed by genomic DNA removal and first-strand cDNA synthesis with TransScript One-Step gDNA Removal and cDNA Synthesis SuperMix. RT-qPCR was conducted using PerfectStart Green qPCR SuperMix on a qTOWER3 G Touch system (Analytik Jena, Jena, Germany). Relative expression was calculated using the $2^{-\Delta\Delta Ct}$ method with *Actin1* as the internal reference [37–39]. Primers are listed in Supplementary Table S2.

2.9. Subcellular Localization Analysis

The full-length coding sequence of *ZmGeBP8* was cloned into pUC19 to construct a pUC19-ZmGeBP8-YFP fusion vector, with empty pUC19-YFP serving as a control. Mesophyll protoplasts were isolated enzymatically from the leaves of yellow maize seedlings and transformed with either construct using PEG–Ca^{2+} mediation. Following a 12–16 h incubation in W5 solution at 25 ± 1 °C in the dark, YFP fluorescence was observed using a confocal laser scanning microscope [40,41].

2.10. Dual-Luciferase Reporter Assay

To test whether *ZmOCL13* regulates the *ZmGeBP8* promoter, a 2.0 kb promoter fragment was cloned upstream of firefly luciferase (LUC) in pGreenII 0800-LUC to generate pGreenII 0800–ZmGeBP8pro. The full-length CDS of *ZmOCL13* was inserted into pCUB to form the pCUB–ZmOCL13 effector. The reporter co-transformed with empty pCUB served as a negative control. Constructs were transformed into *Agrobacterium tumefaciens* strain GV3101. Equal mixtures of reporter and effector bacterial suspensions were infiltrated into leaves of 4–6-week-old *N. benthamiana* plants. Bioluminescence was detected using an in vivo imaging system [42].

3. Results

3.1. Identification of the GeBP Gene Family in Maize

Nineteen *ZmGeBP* genes were identified in the maize genome. Their encoded proteins varied in length and predicted physicochemical properties (Table 1). Protein length ranged from 222 amino acids for ZmGeBP2 to 553 amino acids for ZmGeBP13, corresponding to molecular weights of 23.98–59.88 kDa. The theoretical pI ranged from 4.51 for ZmGeBP7 to 12.56 for ZmGeBP9. All proteins had predicted instability indices above 40, ranging from 41.41 to 99.32. Aliphatic indices ranged from 55.16 to 81.10. GRAVY values were negative for all members and ranged from −1.245 for ZmGeBP15 to −0.321 for ZmGeBP8, indicating predicted hydrophilic properties. Subcellular localization prediction assigned 15 proteins to the nucleus, ZmGeBP5 and ZmGeBP14 to the cytoplasm, and ZmGeBP7 and ZmGeBP19 to chloroplasts.

Table 1. Physicochemical features of *ZmGeBP* gene family members.

Name	ID	Length (aa)	MW (Da)	pI	II	AI	GRAVY	Cell
ZmGeBP1	*Zm00001eb279010_T001*	306	33,172.45	9.71	41.41	70.59	−0.632	nucl
ZmGeBP2	*Zm00001eb213600_T001*	222	23,976.75	8.84	51.87	72.25	−0.661	nucl
ZmGeBP3	*Zm00001eb054670_T001*	362	38,888.29	6.62	75.03	66.35	−0.607	nucl
ZmGeBP4	*Zm00001eb176440_T001*	456	49,715.99	9.53	61.93	64.54	−0.924	nucl
ZmGeBP5	*Zm00001eb264150_T001*	424	46,685.96	9.84	51.58	79.69	−0.637	cyto
ZmGeBP6	*Zm00001eb314630_T001*	428	46,309.48	8.97	59.06	59.67	−0.84	nucl
ZmGeBP7	*Zm00001eb256290_T001*	355	39,338.97	4.51	77.83	57.01	−1.147	chlo
ZmGeBP8	*Zm00001eb018020_T001*	383	40,715.6	5.29	54.1	69.5	−0.321	nucl
ZmGeBP9	*Zm00001eb373390_T001*	329	34,911.3	12.56	99.32	44.13	−0.844	nucl

Table 1. *Cont.*

Name	ID	Length (aa)	MW (Da)	pI	II	AI	GRAVY	Cell
ZmGeBP10	*Zm00001eb100610_T001*	438	47,002.01	9.35	60.08	55.16	−0.931	nucl
ZmGeBP11	*Zm00001eb328650_T001*	374	40,560.59	5.71	70.65	66.36	−0.597	nucl
ZmGeBP12	*Zm00001eb216500_T001*	380	40,810.42	5.74	71.99	67.55	−0.596	nucl
ZmGeBP13	*Zm00001eb203350_T001*	553	59,884.18	8.52	51.24	60.65	−1.033	nucl
ZmGeBP14	*Zm00001eb264080_T001*	419	46,326.48	9.74	52.13	81.1	−0.601	cyto
ZmGeBP15	*Zm00001eb264520_T001*	439	49,243.91	5.23	63.24	55.4	−1.245	nucl
ZmGeBP16	*Zm00001eb394180_T001*	375	40,091.92	5.85	56.53	64.99	−0.402	nucl
ZmGeBP17	*Zm00001eb418630_T001*	270	28,395.81	8.38	41.73	72.85	−0.426	nucl
ZmGeBP18	*Zm00001eb110030_T001*	369	40,016.8	5.8	74.74	66.21	−0.624	nucl
ZmGeBP19	*Zm00001eb256160_T001*	291	31,874.06	10.24	67.85	65.5	−0.724	chlo

3.2. Phylogenetic Analysis of the ZmGeBP Gene Family

To examine the evolutionary relationships of grass GeBP proteins, we constructed a combined phylogenetic tree using sequences from maize, sorghum (*Sorghum bicolor*), and rice (*Oryza sativa*) (Figure 1). The 47 proteins were separated into four major groups, and each group contained representatives from all three species. Group I was the second-largest group and comprised 16 proteins, including 7 ZmGeBPs, 5 SbGeBPs, and 4 OsGeBPs. Group II contained 7 proteins (2 ZmGeBPs, 3 SbGeBPs, and 2 OsGeBPs), while Group III was the largest group, with 17 proteins (7 ZmGeBPs, 3 SbGeBPs, and 7 OsGeBPs). Group IV contained the remaining 7 proteins (3 ZmGeBPs, 2 SbGeBPs, and 2 OsGeBPs). Although homologs from the three grasses were distributed throughout the tree, their unequal representation among the four groups is consistent with lineage-specific changes in family composition after species divergence.

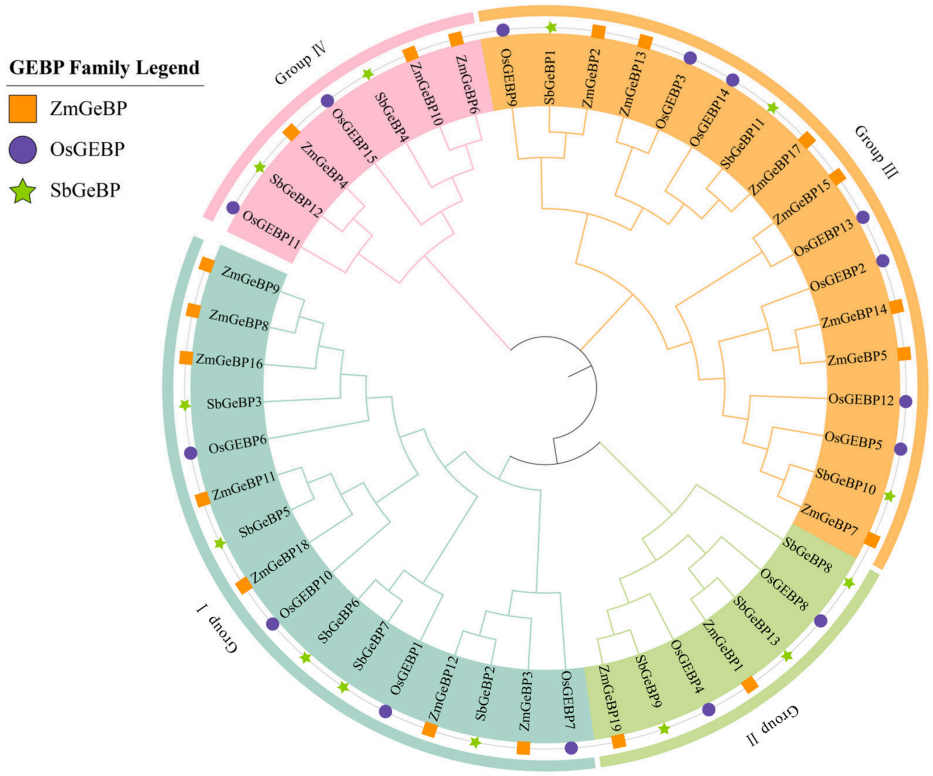

Figure 1. Neighbor-joining phylogenetic tree of GeBP proteins from maize (Zm), sorghum (Sb), and rice (Os). Note: The tree was constructed in MEGA11 with 1000 bootstrap replicates. Clades (Groups I–IV) are distinguished by color, and species origins are marked with distinct symbols.

3.3. Conserved Motifs, Gene Structures, and Tertiary Profiles of ZmGeBP

Phylogenetic analysis divided the 19 maize ZmGeBP proteins into four groups (Figure 2a). MEME analysis identified 10 conserved motifs, designated Motifs 1–10, and individual proteins contained between three and seven motifs (Figure 2b). Motif arrangement was generally more similar among proteins belonging to the same phylogenetic group. Motifs 2 and 1 occurred adjacently in most members of Groups I, II, and IV, whereas proteins in Group III displayed a more variable arrangement. Motif 2 was detected in all 19 proteins, and Motif 3 occurred in 15 members, suggesting that these motifs represent relatively conserved features of the maize GeBP family.

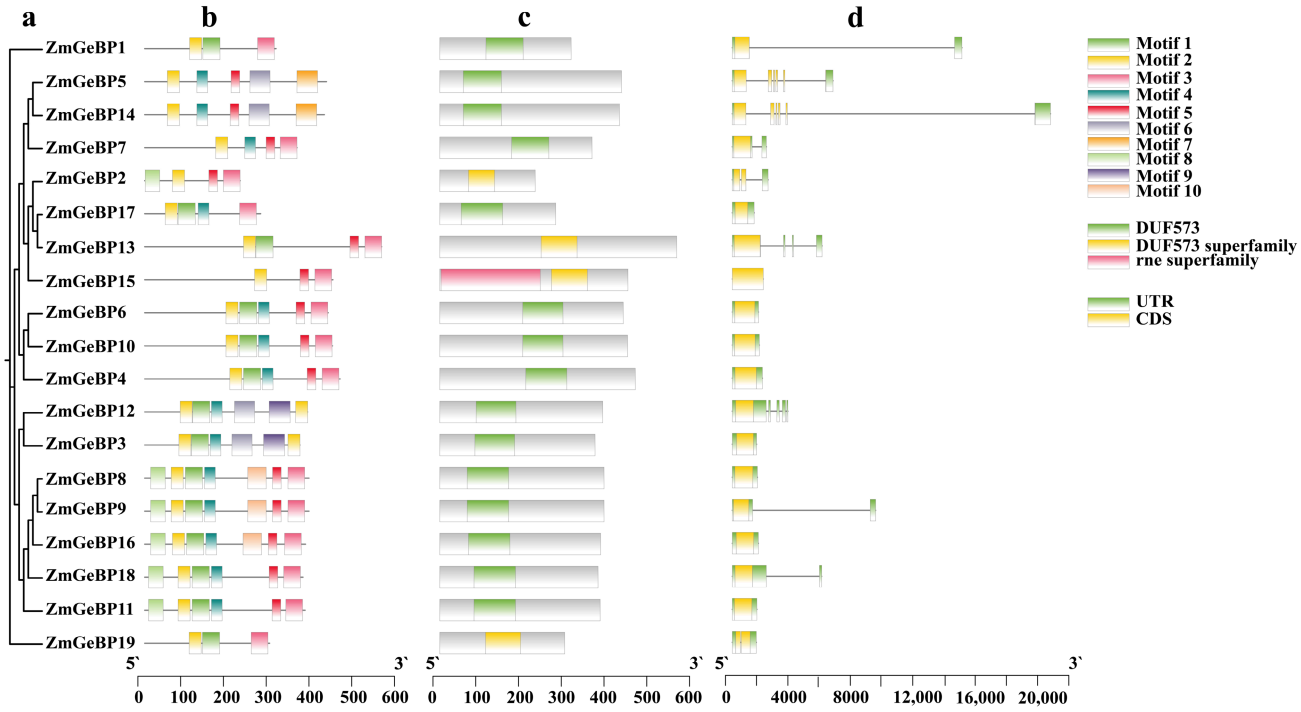

Figure 2. Evolutionary and structural organization of the maize ZmGeBP family. (**a**) Phylogenetic tree of the 19 ZmGEBP proteins. (**b**) Conserved motifs (Motifs 1–10). (**c**) Conserved domain architecture. (**d**) Gene structures: yellow, CDS; green, UTRs; black lines, introns. Note: Motif 1–10 (**b**); DUF573/DUF573 superfamily/rne superfamily (**c**); UTR/CDS (**d**).

Domain composition and exon–intron organization were subsequently examined using the maize genome and its GFF3 annotation (Figure 2c,d). Fifteen family members contained a standard DUF573 domain, whereas ZmGeBP2, ZmGeBP13, ZmGeBP15, and ZmGeBP19 were assigned to the broader DUF573 superfamily. ZmGeBP11 was distinct from the other proteins because it also contained a predicted RNase E superfamily domain. Exon number ranged from one to five among the 19 genes. *ZmGeBP14* contained the longest individual exon, whereas *ZmGeBP2* contained the shortest. Taken together, these results show that the family retains a common domain framework but also exhibits differences in motif composition and gene organization.

Three-dimensional structure prediction showed that the ZmGeBP proteins were predominantly composed of α-helices (Supplementary Figure S2). Most family members contained a central helical bundle accompanied by N- or C-terminal extensions whose length and predicted conformation differed among proteins. Variation was also observed in the number of predicted helices and their packing within the models. These structural predictions complement the motif and domain analyses by showing that the proteins share an overall helical architecture while retaining member-specific structural features.

3.4. Chromosomal Location and Collinearity of ZmGeBP Genes

The 19 *ZmGeBP* genes were mapped to eight of the ten pairs of maize chromosomes and displayed an uneven chromosomal distribution (Supplementary Figure S3). No family member was identified on chromosomes 3 or 8, whereas the other chromosomes contained between one and four genes. Chromosomes 5 and 6 had the largest numbers, with four genes on each chromosome. Chromosomes 1, 2, 4, 7, and 9 each carried two genes, and chromosome 10 contained a single *ZmGeBP* locus. This distribution indicates that family members are dispersed across the maize genome rather than being concentrated within a single chromosomal region.

Segmental duplication analysis identified 11 duplicated paralogous pairs involving 11 *ZmGeBP* loci (Figure 3a). Four genes—*ZmGeBP6*, *ZmGeBP8*, *ZmGeBP10*, and *ZmGeBP11* participated in more than one collinear relationship, suggesting that they occupy recurrent positions within the duplication network. Most duplicated pairs were located on nonhomologous chromosomes, and no prominent tandem-duplication cluster was detected. Within the limits of the present analysis, these results indicate that segmental duplication was the predominant duplication pattern associated with expansion of the maize GeBP family.

To evaluate the evolutionary constraints acting on the duplicated genes, nonsynonymous (Ka) and synonymous (Ks) substitution rates were compared for the 11 segmentally duplicated pairs (Figure 3b). The resulting Ka/Ks ratios ranged from 0.218 to 0.749 and were below 1.0 for every pair. The highest value was observed for the *ZmGeBP10*/*ZmGeBP1* pair (0.749), whereas the *ZmGeBP18*/*ZmGeBP11* pair had the lowest value (0.218). The consistent occurrence of ratios below 1 is compatible with predominantly purifying selection and suggests that duplicated family members have remained under functional constraint following duplication.

Comparative synteny analysis among maize, sorghum, and rice revealed numerous collinear relationships involving GeBP homologs (Figure 4). Syntenic correspondence was more extensive between maize and sorghum, involving 11 of the 19 *ZmGeBP* genes distributed across 7 maize chromosomes. In contrast, fewer collinear relationships were detected between maize and rice, involving only 9 *ZmGeBP* genes on 6 maize chromosomes. This difference is consistent with the closer evolutionary relationship between maize and sorghum and the earlier divergence of the rice lineage.

3.5. Promoter Cis-Element Profiling of ZmGeBP Genes

Analysis of the 2 kb genomic regions upstream of the 19 *ZmGeBP* genes identified 31 types of cis-acting regulatory elements. According to their annotated functions, these elements were divided into four categories: nine light-responsive types, seven types associated with plant growth and development, nine hormone-responsive types, and six stress-responsive types. Both the total number and the diversity of elements differed among family members. *ZmGeBP19* contained the largest total number of predicted sites, with 44 elements, whereas *ZmGeBP16* displayed the greatest element diversity, containing 18 different types (Figure 5a,b).

Light and phytohormone-responsive elements were present in the promoters of all 19 genes, indicating that these two categories were broadly represented across the family. Seven types of biotic and abiotic stress-related elements and six types of growth and development-related elements were also identified; the biotic and abiotic stress-related elements comprised those involved in low-temperature responsiveness, heat stress responsiveness, anaerobic specificity, anaerobic induction, drought induction, multiple stress or developmental regulation, and defense and stress responsiveness. Notably, the promoter of *ZmGeBP17* contained none of the elements of either category, and it was the only family member devoid of all biotic and abiotic stress-related elements, whereas the promoters of

the remaining 18 members each contained at least one such element. Among the growth and development-related elements, *ZmGeBP4*, *ZmGeBP5*, *ZmGeBP17* and *ZmGeBP18* were the only members whose promoters contained none.

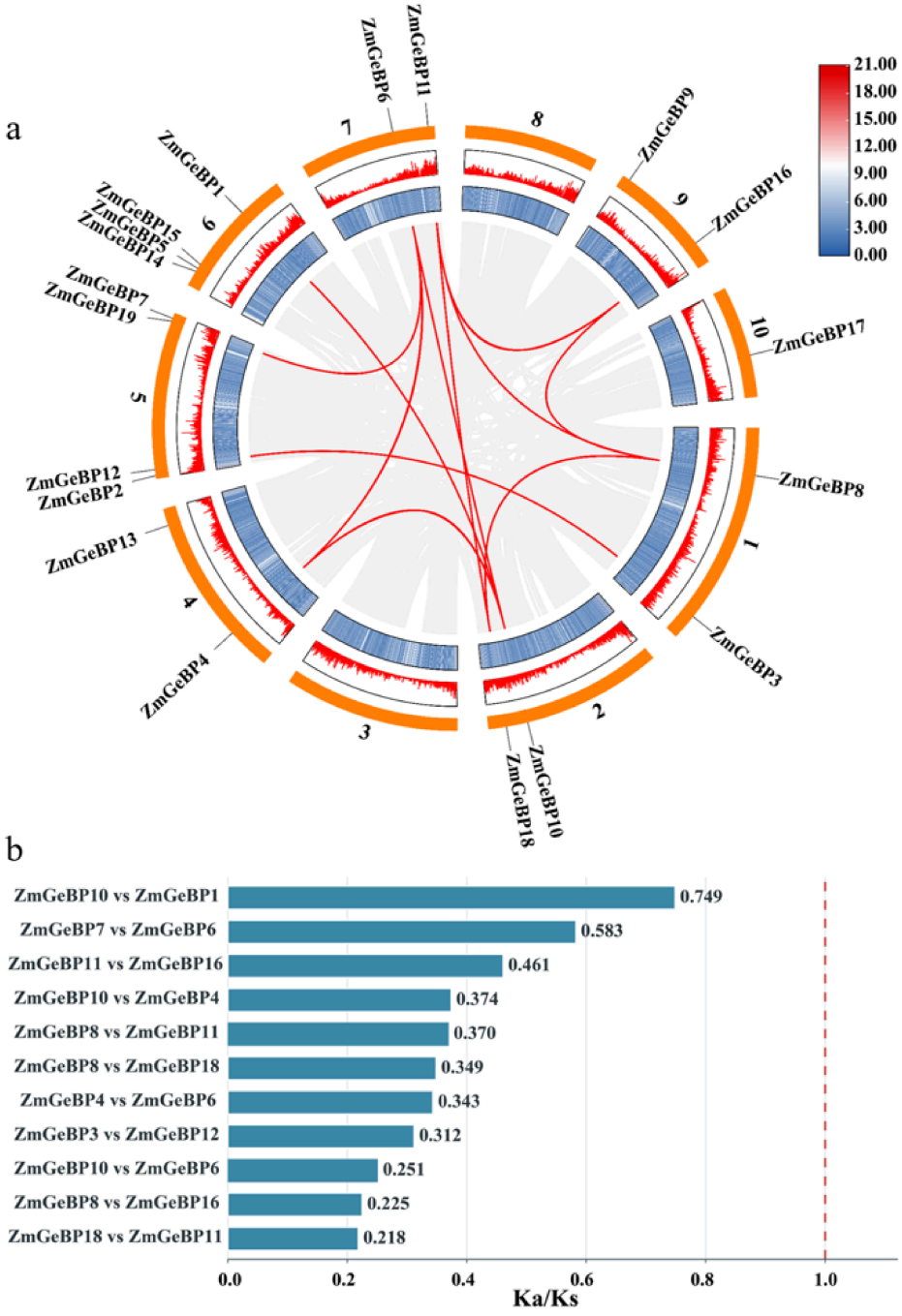

Figure 3. Intragenomic synteny and Ka/Ks ratios of *ZmGeBP* paralogs in maize. (**a**) The gray ribbons in the centre represent collinear blocks within the maize genome and the red curves the collinear gene pairs involving *ZmGeBP* genes; the blue track and red bars represent gene density along each chromosome; the outer orange ring represents the ten maize chromosomes (Chr1–Chr10), numbered 1–10 around the ring. (**b**) Ka/Ks ratios of 11 segmentally duplicated *ZmGeBP* gene pairs. The red dashed line indicates Ka/Ks = 1. Note: The colour scale on the right indicates the range of gene density.

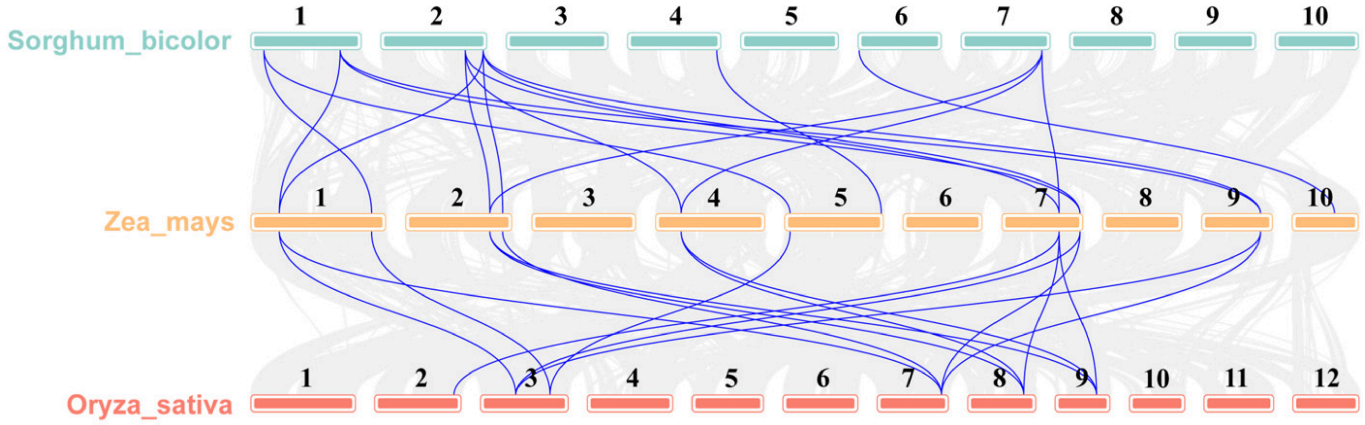

Figure 4. Comparative syntenic alignment of GeBP orthologs among maize, sorghum, and rice. Note: Gray lines represent background collinear blocks across the three genomes; blue lines represent the syntenic GeBP orthologous pairs between maize–sorghum and maize–rice. The numbers above the chromosomes denote the chromosome numbers of sorghum (1–10), maize (1–10) and rice (1–12).

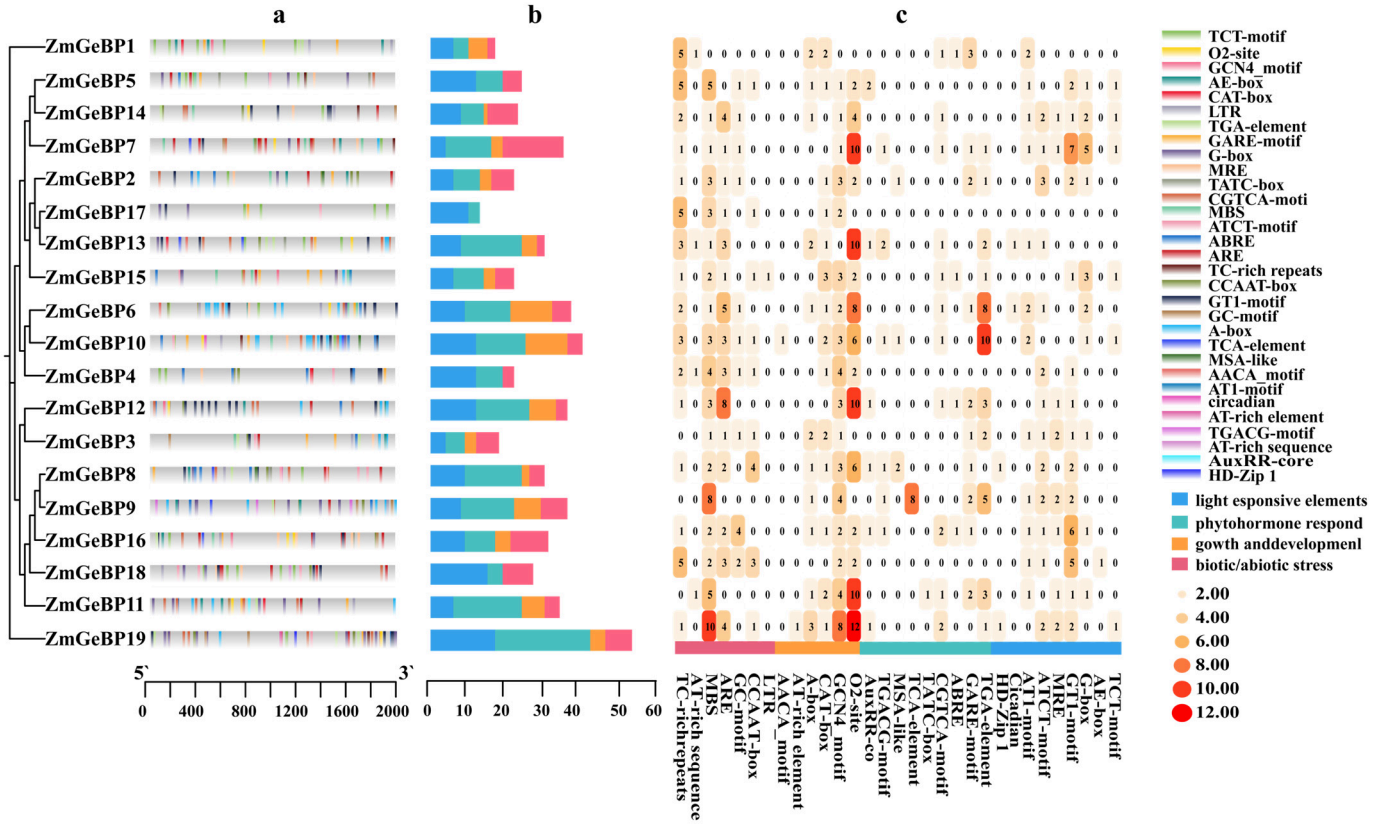

Figure 5. *Cis*-acting regulatory element profiles within 2 kb *ZmGeBP* promoter regions. Note: (**a**) Positions of the predicted elements, with element types indicated by the colour key on the right; (**b**) functional categorization of the identified promoter elements, namely light-responsive, phytohormone-responsive, growth and development-related and biotic and abiotic stress-related elements (colour key on the right); (**c**) element counts per gene, with counts indicated by the colour scale on the right.

3.6. Protein–Protein Interaction Network of ZmGeBP

To examine potential associations involving ZmGeBP proteins, a STRING-based protein–protein association network was constructed (Supplementary Figure S4). The predicted network showed multiple connections among family members, with ZmGeBP1 and ZmGeBP19 displaying the highest node degrees and therefore occupying relatively

central positions in the network topology. Inclusion of the 40 highest-scoring non-family proteins further expanded the network and identified candidate partners that may participate in related physiological processes.

3.7. Tissue-Specific and Stress-Responsive Expression Profiles of ZmGeBP Genes

Reanalysis of public RNA-seq datasets revealed distinct tissue- and stress-dependent expression patterns for *ZmGeBP* genes. In developing tissues, *ZmGeBP7* maintained strong expression in both embryo and endosperm, whereas *ZmGeBP19* transcripts were nearly undetectable in the endosperm, underscoring tissue specificity (Figure 6a). Under environmental stress, *ZmGeBP18* was induced by UV light, *ZmGeBP16* was upregulated during cold exposure, and *ZmGeBP11* was activated by salt treatment. Conversely, heat stress repressed *ZmGeBP4*, *ZmGeBP6*, *ZmGeBP10*, and *ZmGeBP11*. *ZmGeBP8* showed relatively high expression under basal conditions, but was downregulated under multiple abiotic stresses (Figure 6b). Seven representative candidates (*ZmGeBP4*, *6*, *8*, *10*, *11*, *16*, and *18*) were selected for RT-qPCR verification.

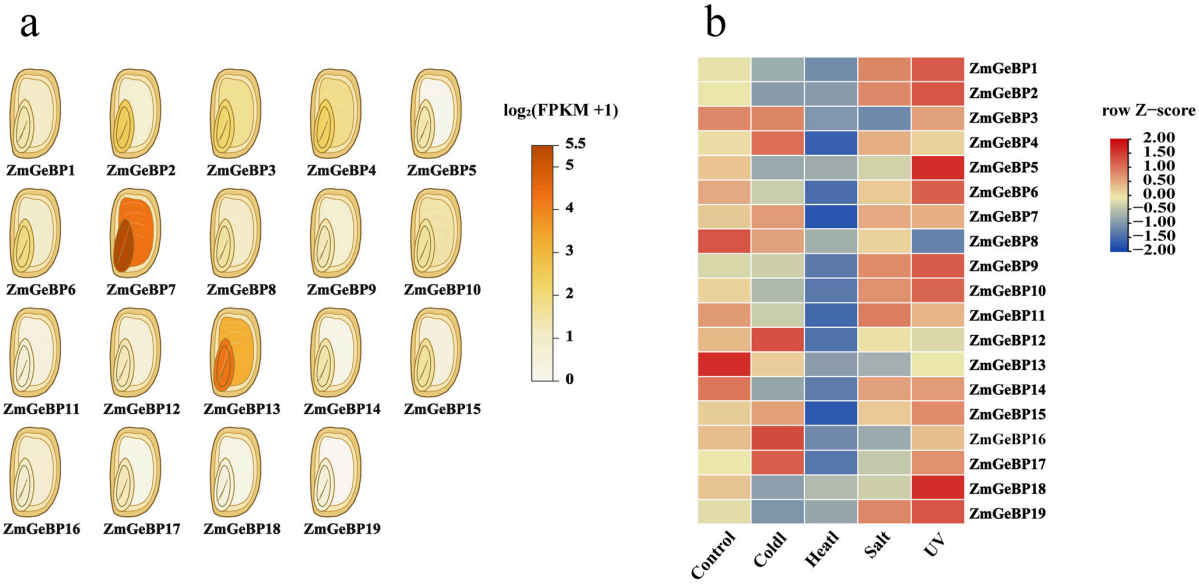

Figure 6. Tissue-specific and abiotic stress expression profiles of maize *ZmGeBP* genes. Note: (**a**) Relative transcript abundance in embryo and endosperm. (**b**) Heatmap of seedling expression under control, cold, heat, salt, and UV conditions.

RT-qPCR validation under artificial seed aging and saline–alkali stress confirmed strong stress responsiveness across candidates (Figure 7a,b). *ZmGeBP4* and *ZmGeBP11* were significantly induced by both stresses, achieving higher fold-changes in the stress-tolerant inbred line Dong 156, with expression peaking at 14–24 h, suggesting that they may have positive regulatory roles in stress tolerance. In contrast, *ZmGeBP10* exhibited stress-dependent duality: it was strongly induced in Dong 156 during seed aging, but preferentially expressed in the sensitive line Dong 237 under saline–alkali stress, with peak divergence occurring at 14–24 h.

Conversely, *ZmGeBP6*, *ZmGeBP8*, *ZmGeBP16*, and *ZmGeBP18* displayed significantly higher induction in the sensitive line Dong 237, peaking at 14–24 h. Among these genes, *ZmGeBP8* displayed the most consistent difference between the two inbred lines: its expression remained comparatively low in Dong 156 but increased markedly in Dong 237 during both artificial seed aging and saline–alkali stress. The reproducibility of this genotype-dependent pattern led us to select *ZmGeBP8* for further characterization as a candidate associated with stress sensitivity.

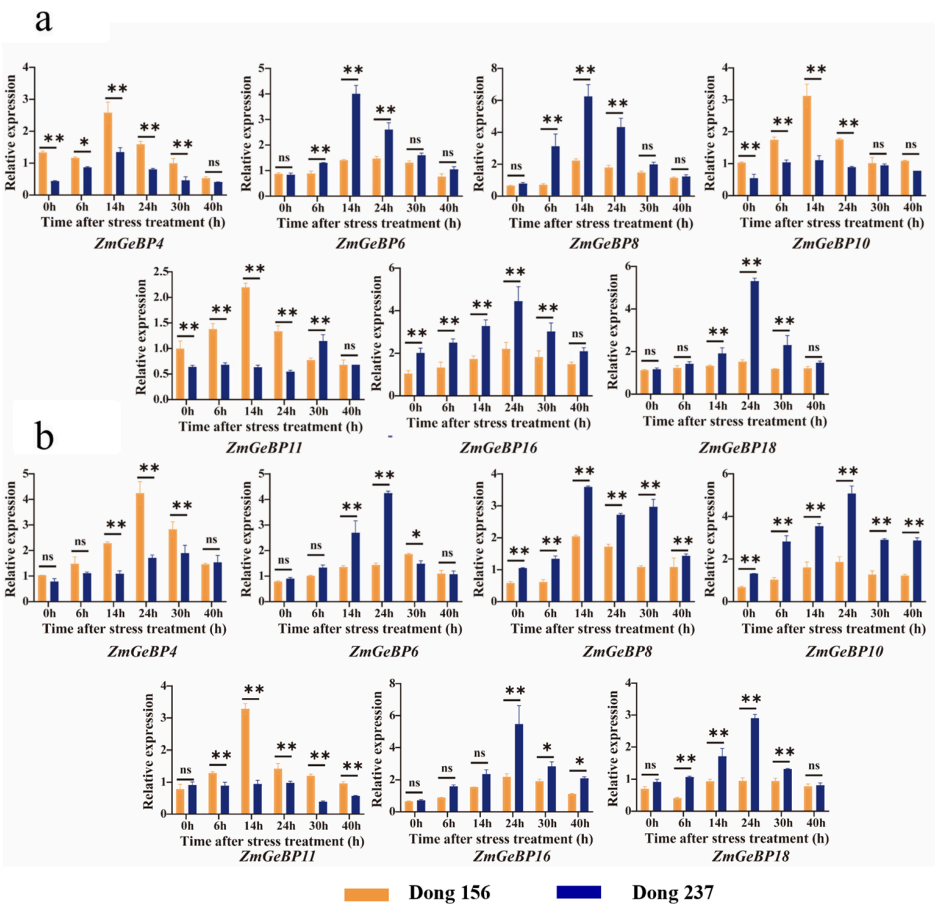

Figure 7. Quantitative RT-qPCR expression dynamics of *ZmGeBP* genes under stress. (**a**) Expression in inbred lines Dong 156 (tolerant) and Dong 237 (sensitive) during artificial seed aging. (**b**) Expression profiles under saline–alkali stress. Note: Orange and blue bars denote Dong 156 and Dong 237, respectively (* $p < 0.05$, ** $p < 0.01$; ns, non-significant).

3.8. Subcellular Localization of ZmGeBP8

Transient expression of a ZmGeBP8–YFP fusion construct in maize mesophyll protoplasts localized the fluorescent signal exclusively to the nucleus (Figure 8). This nuclear restriction aligns with its predicted role as a functional transcription factor.

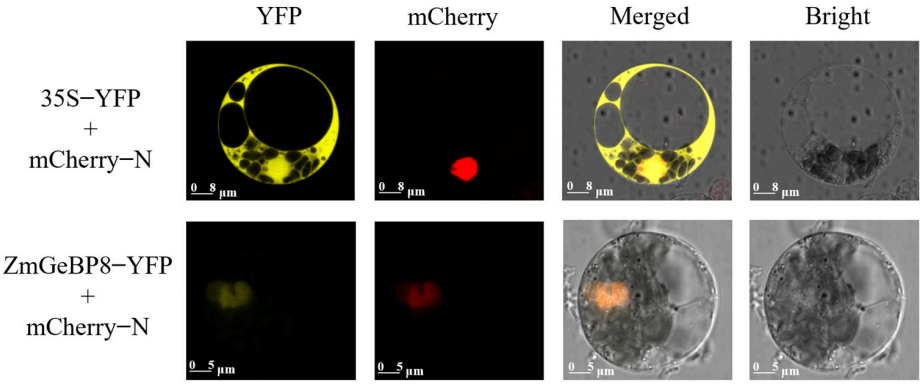

Figure 8. Subcellular localization of ZmGeBP8–YFP fusion protein in maize mesophyll protoplasts. Note: *ZmGEBP8* was fused to YFP (pUC19-35S-ZmGEBP8-YFP) and co-transfected with the nuclear marker mCherry-N into maize mesophyll protoplasts, with free YFP (pUC19-35S-YFP) as the control. Columns show the YFP channel, the mCherry channel, the merged image and the bright field image. The YFP signal is shown in yellow and the mCherry signal in red; the merged images show the overlay of the two channels. bar = 8 μm (upper panels) and 5 μm (lower panels).

3.9. Upstream Transcriptional Regulation of ZmGeBP8 by ZmOCL13

Promoter analysis via PlantTFDB identified *ZmOCL13*, an HD-ZIP IV transcription factor, as a candidate upstream regulator binding the *ZmGeBP8* promoter. Under stress conditions, In dual-luciferase reporter assays, co-expressing *ZmOCL13* significantly repressed *ZmGeBP8* promoter-driven luciferase activity compared with the empty vector control (Figure 9a–c). RT-qPCR confirmed that *ZmOCL13* was significantly upregulated in the tolerant line Dong 156 (Figure 9d,e). Together, suggest that *ZmOCL13* may potentially participate in the transcriptional regulation of *ZmGeBP8* during stress responses in maize.

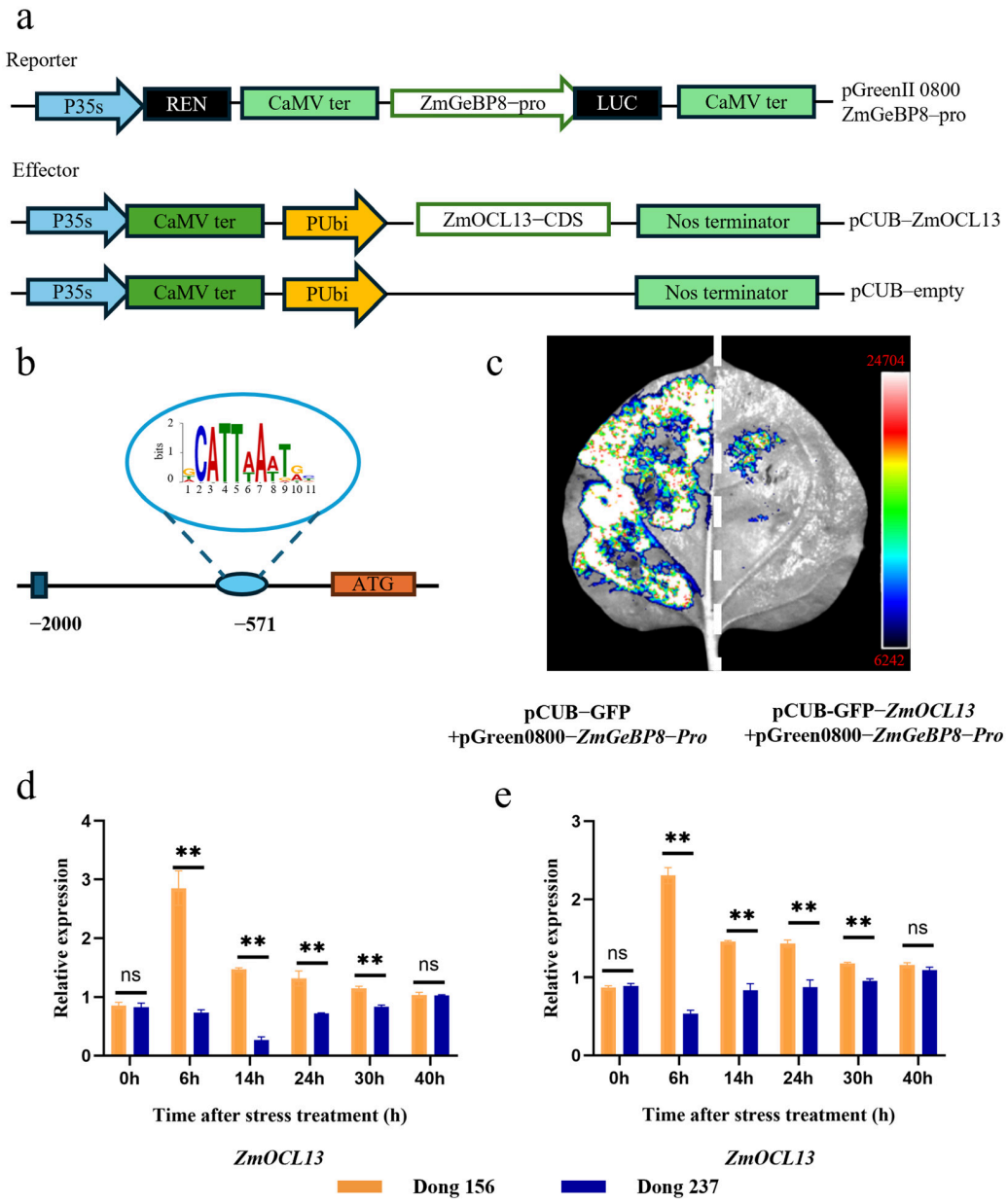

Figure 9. Transcriptional repression of *ZmGeBP8* by *ZmOCL13* and stress expression dynamics. (**a**) Dual-luciferase reporter construct schematics. (**b**) Map of the 2000 bp *ZmGeBP8* promoter region showing the predicted HD-ZIP IV binding motif at −571 bp. (**c**) Transient dual-luciferase activity imaging in *Nicotiana benthamiana* leaves. (**d**,**e**) Relative expression of *ZmOCL13* under artificial seed aging (**d**) and saline–alkali stress (**e**). Note: Orange and blue bars represent Dong 156 and Dong 237, respectively (** $p < 0.01$; ns, non-significant).

4. Discussion

When facing adverse environments, plants undergo massive transcriptional reprogramming driven by complex transcription factor networks to balance growth and stress adaptation [4,43]. GLABROUS1 ENHANCER-BINDING PROTEIN (GeBP) family members harbor a noncanonical leucine-zipper motif alongside a distinct DNA-binding domain [9]. Prior studies show that GeBP and GeBP-like proteins participate in cytokinin signaling, tissue morphogenesis, and abiotic stress responses [10,11,44]. Although GeBP genes have been identified in maize as part of a comparative analysis of grasses, their responses to artificial seed aging and saline–alkali stress, and the roles of individual members in these processes, remain poorly characterized [19]. Here, we combined genome-wide bioinformatic and comparative genomic analyses with spatiotemporal expression profiling and preliminary regulatory assays to further characterize the maize ZmGeBP family and identify stress-responsive candidates, providing a basis for future functional studies and genetic improvement in maize.

Genome-wide scanning identified 19 *ZmGeBP* genes in maize, which resolved into four phylogenetic clades (Figure 1). Clade size variations align with patterns in other Poaceae species, pointing to shared evolutionary mechanisms underlying GeBP expansion in grasses [19]. Conserved motif arrangements and exon–intron architectures differed distinctly among clades, signaling functional diversification. Subclade-specific gene structures suggest that evolutionary divergence of *ZmGeBP* paralogs facilitated neofunctionalization following duplication events [45]. Furthermore, 3D structural modeling predicted that ZmGeBP proteins combine conserved helical bundles with flexible intrinsically disordered tails, an architecture consistent with potential roles in transcriptional regulation [9].

Expansion of plant gene families can occur through tandem duplication, segmental duplication, and transposition [46]. In the present analysis, 11 segmentally duplicated pairs were identified among the maize *ZmGeBP* genes, whereas no prominent tandem-duplication cluster was detected. Segmental duplication therefore represented the predominant duplication pattern associated with this family, which is broadly consistent with observations in wheat and upland cotton [8,19,47]. All duplicated pairs had Ka/Ks ratios below 1, suggesting that purifying selection has acted on these genes after duplication. Comparative synteny was more extensive between maize and sorghum than between maize and rice, in agreement with their established phylogenetic relationships [48]. Promoter analysis additionally identified numerous hormone- and stress-responsive cis-elements [49–51] including elements associated with auxin, gibberellin, abscisic acid (ABA), methyl jasmonate, cytokinin, salicylic acid, cold, drought, hypoxia, and defense responses. Similar enrichment has been reported in wheat [8], *Brassica rapa* [12], and soybean [18]. Hormone signaling is closely integrated with plant stress responses [52]: type-B ARRs suppress ABA signaling, whereas type-A ARRs can promote ABA-dependent drought tolerance [53]; *OsCPN10a* contributes to rice seed storability through ABA homeostasis and restriction of ROS accumulation [54]; and jasmonate-mediated degradation of JAZ8 releases an NF-Y complex that activates salt-responsive genes in *Arabidopsis* [55]. Therefore, the promoter profiles observed here may be associated with the involvement of *ZmGeBP* genes in stress-related signaling.

Transcriptional shifts under environmental challenges help identify key resistance candidates [4]. Our RT-qPCR experiments, together with reanalysis of MaizeGDB transcriptome data [56], revealed divergent *ZmGeBP* expression profiles during seed aging and saline–alkali stress. In the tolerant line Dong 156, *ZmGeBP4* and *ZmGeBP11*, which may have positive regulatory roles, were strongly induced. In contrast, susceptible Dong 237 accumulated *ZmGeBP6*, *ZmGeBP16*, and *ZmGeBP18*, reflecting injury-induced passive stress responses. *ZmGeBP8* showed the most pronounced genotype-dependent pattern, being suppressed in Dong 156 but heavily induced in Dong 237, marking it as a negative regulator of stress tolerance. Molecular assays confirmed that the HD-ZIP IV transcription factor *ZmOCL13* directly binds and re-

presses the *ZmGeBP8* promoter. HD-ZIP IV OCL proteins act as epidermal sensors that govern environmental adaptation [57–59], and maize HD-ZIP family members are known drivers of abiotic stress tolerance [60]. For instance, *ZmHDZ9* overexpression enhances drought tolerance, whereas dominant-negative *OCL1* retards kernel development [60,61].

Based on these findings, we propose a regulatory model governing maize tolerance to seed aging and saline–alkali stress (Supplementary Figure S5). Under stress, elevated *ZmOCL13* in tolerant maize lines directly represses the negative regulator *ZmGeBP8*, mitigating its adverse effects and enhancing stress tolerance. In sensitive lines, lower *ZmOCL13* levels allow *ZmGeBP8* accumulation, impairing stress defenses and worsening cellular damage. The *ZmOCL13*–*ZmGeBP8* regulatory module identified in the present study provides candidate targets for further investigation of maize seed storability and stress tolerance.

5. Conclusions

We identified 19 *ZmGeBP* genes and classified their encoded proteins into four phylogenetic groups together with homologs from sorghum and rice. Duplication and synteny analyses showed that segmental duplication was the predominant duplication pattern detected in maize and that collinear relationships were retained among the three grasses. The *ZmGeBP* promoters contained cis-acting elements associated with development, light, phytohormone responses, and stress. RT-qPCR analysis of seven selected genes revealed temporal and genotype-dependent expression patterns during artificial seed aging and saline–alkali stress. Nuclear localization supported the transcriptional regulatory function of *ZmGeBP8*, and dual-luciferase assays indicated that *ZmOCL13* represses *ZmGeBP8* promoter activity. These findings provide candidate genes and a molecular framework for elucidating *ZmGeBP8* mediated stress responses and improving stress resilience in maize.

Supplementary Materials: The following supporting information can be downloaded at https://www.mdpi.com/article/10.3390/agronomy16212100/s1. Supplementary Figure S1. Comparison of relative germination performance between Dong156 and Dong237 under artificial seed aging and saline–alkali stress. Supplementary Figure S2. Predicted 3D tertiary structures of the 19 maize ZmGeBP proteins. Supplementary Figure S3. Genomic distribution and chromosomal mapping of *ZmGeBP* genes in maize. Supplementary Figure S4. Predicted protein–protein interaction network of maize ZmGeBP family members and candidate interactor partners. Supplementary Figure S5. Proposed *ZmOCL13*–*ZmGeBP8* module regulating maize tolerance to seed aging and saline–alkali stress. Supplementary Table S1. GeBP protein sequences from maize (*Zea mays*), sorghum (*Sorghum bicolor*), and rice (*Oryza sativa*) used for phylogenetic analysis. Supplementary Table S2. Primer sequences used for RT-qPCR analysis of *ZmGeBP* gene expression.

Author Contributions: The authors confirm their contributions to the paper as follows: study conception and design: C.L. and H.D.; experimental investigation: J.W., M.W. and Y.L.; data analysis: Q.M., Y.Z. (Yuyang Zhou), Y.S. and H.L.; guidance on manuscript preparation: L.Z., Y.Z. (Yu Zhou), X.Z. and Z.W.; draft manuscript preparation: J.W. and M.W. All authors have read and agreed to the published version of the manuscript.

Funding: This research was supported by the National Natural Science Foundation of China (NSFC; grant no. 32472199).

Data Availability Statement: The publicly available RNA-seq datasets analyzed in this study were obtained from MaizeGDB. The RNA-seq data used for the tissue-specific expression analysis of maize embryos and endosperms are available in the National Center for Biotechnology Information (NCBI) under accession numbers PRJNA171684 and SRP010680. The RNA-seq data used for the abiotic stress expression analysis, including cold, heat, salt, and ultraviolet treatments, are available under NCBI BioProject accession PRJNA244661. All other data supporting the findings of this study are available within the article and its Supplementary Information. Additional data are available from the corresponding author upon reasonable request.

Conflicts of Interest: The authors declare no conflicts of interest.

References

1. Erenstein, O.; Jaleta, M.; Sonder, K.; Mottaleb, K.; Prasanna, B.W. Global maize production, consumption and trade: Trends and R&D implications. *Food Secur.* **2022**, *14*, 1295–1319. [CrossRef]
2. Reed, R.C.; Bradford, K.J.; Khanday, I. Seed germination and vigor: Ensuring crop sustainability in a changing climate. *Heredity* **2022**, *128*, 450–459. [CrossRef]
3. Zhou, W.; Chen, F.; Luo, X.; Dai, Y.; Yang, Y.; Zheng, C.; Yang, W.; Shu, K. A matter of life and death: Molecular, physiological, and environmental regulation of seed longevity. *Plant Cell Environ.* **2020**, *43*, 293–302. [CrossRef]
4. Zhang, H.; Zhu, J.; Gong, Z.; Zhu, J.-K. Abiotic stress responses in plants. *Nat. Rev. Genet* **2022**, *23*, 104–119. [CrossRef]
5. Wang, H.; Wang, H.; Shao, H.; Tang, X. Recent Advances in Utilizing Transcription Factors to Improve Plant Abiotic Stress Tolerance by Transgenic Technology. *Front. Plant Sci.* **2016**, *7*, 67. [CrossRef]
6. Sheshadri, S.A.; Nishanth, M.J.; Simon, B. Stress-Mediated cis-Element Transcription Factor Interactions Interconnecting Primary and Specialized Metabolism in planta. *Front. Plant Sci.* **2016**, *7*, 1725. [CrossRef]
7. Hrmova, M.; Hussain, S.S. Plant Transcription Factors Involved in Drought and Associated Stresses. *Int. J. Mol. Sci.* **2021**, *22*, 5662. [CrossRef]
8. Zhang, S.; Ding, J.; Li, T.; Zhao, Y.; Xu, D.; Zeng, J.; Liu, W.; Qu, M.; Ma, W.; Dai, X. Comprehensive Updated Genome-Wide Identification and Expression Patterns of the TaGeBP Gene Family in Wheat. *Int. J. Mol. Sci.* **2025**, *26*, 11972. [CrossRef]
9. Curaba, J.; Herzog, M.; Vachon, G. GeBP, the first member of a new gene family in Arabidopsis, encodes a nuclear protein with DNA-binding activity and is regulated by KNAT1. *Plant J.* **2003**, *33*, 305–317. [CrossRef]
10. Chevalier, F.; Perazza, D.; Laporte, F.; Le Hénanff, G.; Hornitschek, P.; Bonneville, J.-M.; Herzog, M.; Vachon, G. GeBP and GeBP-like proteins are noncanonical leucine-zipper transcription factors that regulate cytokinin response in Arabidopsis. *Plant Physiol.* **2008**, *146*, 1142–1154. [CrossRef]
11. Khare, D.; Mitsuda, N.; Lee, S.; Song, W.-Y.; Hwang, D.; Ohme-Takagi, M.; Martinoia, E.; Lee, Y.; Hwang, J.-U. Root avoidance of toxic metals requires the GeBP-LIKE 4 transcription factor in *Arabidopsis thaliana*. *New Phytol.* **2017**, *213*, 1257–1273. [CrossRef]
12. Wang, R.; Wu, X.; Wang, Z.; Zhang, X.; Chen, L.; Duan, Q.; Huang, J. Genome-Wide Identification and Expression Analysis of BrGeBP Genes Reveal Their Potential Roles in Cold and Drought Stress Tolerance in *Brassica rapa*. *Int. J. Mol. Sci.* **2023**, *24*, 13597. [CrossRef]
13. Liu, R.-X.; Li, H.-L.; Qiao, Z.-W.; Liu, H.-F.; Zhao, L.-L.; Wang, X.-F.; Zhang, Z.; Zhang, S.; Song, L.-Q.; You, C.-X. Genome-wide analysis of MdGeBP family and functional identification of MdGeBP3 in *Malus domestica*. *Environ. Exp. Bot.* **2023**, *208*, 105262. [CrossRef]
14. Song, Y.; Yu, J.; Xu, Y.; Wang, J.; Wang, M.; Wang, J.; Jia, Y.; Li, C.; Xing, J.; Zhou, Y.; et al. Integrative Physiology, Transcriptome, and Metabolome Analysis Reveals Pathways and the Key Gene ZmARF27 Involved in Vigor Loss during Artificial Aging of Maize Seeds. *J. Agric. Food Chem.* **2025**, *73*, 15993–16010. [CrossRef]
15. Wang, C.; Wei, X.; Wang, Y.; Wu, C.; Jiao, P.; Jiang, Z.; Liu, S.; Ma, Y.; Guan, S. Metabolomics and Transcriptomic Analysis Revealed the Response Mechanism of Maize to Saline-Alkali Stress. *Plant Biotechnol. J.* **2025**, *23*, 5397–5416. [CrossRef]
16. Song, Y.; Lv, Z.; Wang, Y.; Li, C.; Jia, Y.; Zhu, Y.; Cao, M.; Zhou, Y.; Zeng, X.; Wang, Z.; et al. Identification of miRNAs Mediating Seed Storability of Maize during Germination Stage by High-Throughput Sequencing, Transcriptome and Degradome Sequencing. *Int. J. Mol. Sci.* **2022**, *23*, 12339. [CrossRef]
17. Divya, D.; Kim, C.-K.; Cho, L.-H.; Kim, D.; Lee, D.-J.; Rahman, M.; Sahu, N.; Jeon, J.-S.; Chung, M.-Y. Genome-wide characterization and expression profiling of GeBP gene family members in response to four abiotic stresses and ABA hormone treatment in tomato (*Solanum lycopersicum* L.). *3 Biotech* **2025**, *15*, 402. [CrossRef]
18. Liu, S.; Liu, Y.; Liu, C.; Zhang, F.; Wei, J.; Li, B. Genome-Wide Characterization and Expression Analysis of GeBP Family Genes in Soybean. *Plants* **2022**, *11*, 1848. [CrossRef]
19. Huang, J.; Zhang, Q.; He, Y.; Liu, W.; Xu, Y.; Liu, K.; Xian, F.; Li, J.; Hu, J. Genome-Wide Identification, Expansion Mechanism and Expression Profiling Analysis of GLABROUS1 Enhancer-Binding Protein (GeBP) Gene Family in Gramineae Crops. *Int. J. Mol. Sci.* **2021**, *22*, 8758. [CrossRef]
20. Draves, M.A.; Muench, R.L.; Lang, M.G.; Kelley, D.R. Maize Seedling Growth and Hormone Response Assays Using the Rolled Towel Method. *Curr. Protoc.* **2022**, *2*, e562. [CrossRef]
21. da Silva, M.B.P.; Coelho, C.M.M.; Siega, Y.P. Evaluation of biochemical component determinants for superior seedling performance in high-vigor maize seeds under accelerated aging stress. *Bragantia* **2024**, *83*, e20230297. [CrossRef]
22. Hu, Y.; Li, C.; Zhou, R.; Song, Y.; Lv, Z.; Wang, Q.; Dong, X.; Liu, S.; Feng, C.; Zhou, Y.; et al. The Transcription Factor ZmNAC89 Gene Is Involved in Salt Tolerance in Maize (*Zea mays* L.). *Int. J. Mol. Sci.* **2023**, *24*, 15099. [CrossRef]

23. Jin, J.; Tian, F.; Yang, D.-C.; Meng, Y.-Q.; Kong, L.; Luo, J.; Gao, G. PlantTFDB 4.0: Toward a central hub for transcription factors and regulatory interactions in plants. *Nucleic Acids Res.* **2017**, *45*, D1040–D1045. [CrossRef]
24. Duvaud, S.; Gabella, C.; Lisacek, F.; Stockinger, H.; Ioannidis, V.; Durinx, C. Expasy, the Swiss Bioinformatics Resource Portal, as designed by its users. *Nucleic Acids Res.* **2021**, *49*, W216–W227. [CrossRef]
25. Portwood, J.L., II; Woodhouse, M.R.; Cannon, E.K.; Gardiner, J.M.; Harper, L.C.; Schaeffer, M.L.; Walsh, J.R.; Sen, T.Z.; Cho, K.T.; Schott, D.A.; et al. MaizeGDB 2018: The maize multi-genome genetics and genomics database. *Nucleic Acids Res.* **2019**, *47*, D1146–D1154. [CrossRef]
26. Tamura, K.; Stecher, G.; Kumar, S. MEGA11: Molecular Evolutionary Genetics Analysis Version 11. *Mol. Biol. Evol.* **2021**, *38*, 3022–3027. [CrossRef]
27. Letunic, I.; Bork, P. Interactive Tree Of Life (iTOL) v5: An online tool for phylogenetic tree display and annotation. *Nucleic Acids Res.* **2021**, *49*, W293–W296. [CrossRef]
28. Nystrom, S.L.; McKay, D.J. Memes: A motif analysis environment in R using tools from the MEME Suite. *PLoS Comput. Biol.* **2021**, *17*, e1008991. [CrossRef]
29. Chen, C.; Wu, Y.; Li, J.; Wang, X.; Zeng, Z.; Xu, J.; Liu, Y.; Feng, J.; Chen, H.; He, Y.; et al. TBtools-II: A "one for all, all for one" bioinformatics platform for biological big-data mining. *Mol. Plant* **2023**, *16*, 1733–1742. [CrossRef]
30. Abramson, J.; Adler, J.; Dunger, J.; Evans, R.; Green, T.; Pritzel, A.; Ronneberger, O.; Willmore, L.; Ballard, A.J.; Bambrick, J.; et al. Accurate structure prediction of biomolecular interactions with AlphaFold 3. *Nature* **2024**, *630*, 493–500. [CrossRef]
31. Wang, Y.; Tang, H.; Wang, X.; Sun, Y.; Joseph, P.V.; Paterson, A.H. Detection of colinear blocks and synteny and evolutionary analyses based on utilization of MCScanX. *Nat. Protoc.* **2024**, *19*, 2206–2229. [CrossRef]
32. Zhang, Z. KaKs_Calculator 3.0: Calculating Selective Pressure on Coding and Non-Coding Sequences. *Genom. Proteom. Bioinform.* **2022**, *20*, 536–540. [CrossRef]
33. Chow, C.N.; Yang, C.W.; Wu, N.Y.; Wang, H.T.; Tseng, K.C.; Chiu, Y.H.; Lee, T.Y.; Chang, W.C. PlantPAN 4.0: Updated Database for Identifying Conserved Non-Coding Sequences and Exploring Dynamic Transcriptional Regulation in Plant Promoters. *Nucleic Acids Res.* **2024**, *52*, D1569–D1578. [CrossRef]
34. Szklarczyk, D.; Nastou, K.; Koutrouli, M.; Kirsch, R.; Mehryary, F.; Hachilif, R.; Hu, D.; Peluso, M.E.; Huang, Q.; Fang, T.; et al. The STRING database in 2025: Protein networks with directionality of regulation. *Nucleic Acids Res.* **2024**, *53*, D730–D737. [CrossRef]
35. Waters, A.J.; Makarevitch, I.; Noshay, J.; Burghardt, L.T.; Hirsch, C.N.; Hirsch, C.D.; Springer, N.M. Natural variation for gene expression responses to abiotic stress in maize. *Plant J.* **2017**, *89*, 706–717. [CrossRef]
36. Stelpflug, S.C.; Sekhon, R.S.; Vaillancourt, B.; Hirsch, C.N.; Buell, C.R.; de Leon, N.; Kaeppler, S.M. An Expanded Maize Gene Expression Atlas based on RNA Sequencing and its Use to Explore Root Development. *Plant Genome* **2016**, *9*, plantgenome2015.04.0025. [CrossRef]
37. Bustin, S.A.; Ruijter, J.M.; van den Hoff, M.J.B.; Kubista, M.; Pfaffl, M.W.; Shipley, G.L.; Tran, N.; Rödiger, S.; Untergasser, A.; Mueller, R.; et al. MIQE 2.0: Revision of the Minimum Information for Publication of Quantitative Real-Time PCR Experiments Guidelines. *Clin. Chem.* **2025**, *71*, 634–651. [CrossRef]
38. Alves Oliveira, D.; Tang, J.D.; Warburton, M.L. Reference Gene Selection for RT-qPCR Analysis in Maize Kernels Inoculated with Aspergillus flavus. *Toxins* **2021**, *13*, 386. [CrossRef]
39. Vennapusa, A.R.; Somayanda, I.M.; Doherty, C.J.; Jagadish, S.V.K. A universal method for high-quality RNA extraction from plant tissues rich in starch, proteins and fiber. *Sci. Rep.* **2020**, *10*, 16887. [CrossRef]
40. Tonnies, J.; Mueth, N.A.; Gorjifard, S.; Chu, J.; Queitsch, C. Scalable Transfection of Maize Mesophyll Protoplasts. *J. Vis. Exp.* **2023**, *196*, e64991. [CrossRef]
41. Gao, L.; Shen, G.; Zhang, L.; Qi, J.; Zhang, C.; Ma, C.; Li, J.; Wang, L.; Malook, S.U.; Wu, J. An efficient system composed of maize protoplast transfection and HPLC-MS for studying the biosynthesis and regulation of maize benzoxazinoids. *Plant Methods* **2019**, *15*, 144. [CrossRef]
42. Norkunas, K.; Harding, R.; Dale, J.; Dugdale, B. Improving agroinfiltration-based transient gene expression in *Nicotiana benthamiana*. *Plant Methods* **2018**, *14*, 71. [CrossRef]
43. Baillo, E.H.; Kimotho, R.N.; Zhang, Z.; Xu, P. Transcription Factors Associated with Abiotic and Biotic Stress Tolerance and Their Potential for Crops Improvement. *Genes* **2019**, *10*, 771. [CrossRef]
44. Kieber, J.J.; Schaller, G.E. Cytokinin signaling in plant development. *Development* **2018**, *145*, dev149344. [CrossRef]
45. Panchy, N.; Lehti-Shiu, M.; Shiu, S.-H. Evolution of Gene Duplication in Plants. *Plant Physiol.* **2016**, *171*, 2294–2316. [CrossRef]
46. Qiao, X.; Li, Q.; Yin, H.; Qi, K.; Li, L.; Wang, R.; Zhang, S.; Paterson, A.H. Gene duplication and evolution in recurring polyploidization–diploidization cycles in plants. *Genome Biol.* **2019**, *20*, 38. [CrossRef]
47. Wu, J.; Liu, R.; Xie, Y.; Zhao, S.; Yan, M.; Sun, N.; Zhan, Y.; Li, F.; Yu, S.; Feng, Z.; et al. Association of GhGeBP genes with fiber quality and early maturity related traits in upland cotton. *BMC Genom.* **2024**, *25*, 1058. [CrossRef]
48. Liu, D.; Hunt, M.; Tsai, I.J. Inferring synteny between genome assemblies: A systematic evaluation. *BMC Bioinform.* **2018**, *19*, 26. [CrossRef]

49. Ho, C.L.; Geisler, M. Genome-Wide Computational Identification of Biologically Significant Cis-Regulatory Elements and Associated Transcription Factors from Rice. *Plants* **2019**, *8*, 441. [CrossRef]
50. Kong, W.; Ding, L.; Cheng, J.; Wang, B. Identification and expression analysis of genes with pathogen-inducible cis-regulatory elements in the promoter regions in *Oryza sativa*. *Rice* **2018**, *11*, 52. [CrossRef]
51. Sarwar, R.; Jiang, T.; Ding, P.; Gao, Y.; Tan, X.; Zhu, K. Genome-wide analysis and functional characterization of the DELLA gene family associated with stress tolerance in *B. napus*. *BMC Plant Biol.* **2021**, *21*, 286. [CrossRef]
52. Waadt, R.; Seller, C.A.; Hsu, P.-K.; Takahashi, Y.; Munemasa, S.; Schroeder, J.I. Plant hormone regulation of abiotic stress responses. *Nat. Rev. Mol. Cell Biol.* **2022**, *23*, 680–694. [CrossRef]
53. Huang, X.; Hou, L.; Meng, J.; You, H.; Li, Z.; Gong, Z.; Yang, S.; Shi, Y. The Antagonistic Action of Abscisic Acid and Cytokinin Signaling Mediates Drought Stress Response in Arabidopsis. *Mol. Plant* **2018**, *11*, 970–982. [CrossRef]
54. Liao, S.; Wei, Y.; Zhu, Y.; Li, K.; Chen, T.; Zhao, S.; Wu, F.; Wang, J.; Yu, P.; Xie, H.; et al. OsCPN10a, cooperating with OsCPN20 and OsHSP60-3B negatively regulate ABA signaling and enhance seed storability in rice. *J. Integr. Plant Biol.* **2026**, *68*, 2242–2263. [CrossRef]
55. Li, X.; Li, C.; Shi, L.; Lv, G.; Li, X.; Liu, Y.; Jia, X.; Liu, J.; Chen, Y.; Zhu, L.; et al. Jasmonate signaling pathway confers salt tolerance through a NUCLEAR FACTOR-Y trimeric transcription factor complex in Arabidopsis. *Cell Rep.* **2024**, *43*, 113825. [CrossRef]
56. Hoopes, G.M.; Hamilton, J.P.; Wood, J.C.; Esteban, E.; Pasha, A.; Vaillancourt, B.; Provart, N.J.; Buell, C.R. An updated gene atlas for maize reveals organ-specific and stress-induced genes. *Plant J.* **2019**, *97*, 1154–1167. [CrossRef]
57. Sharif, R.; Raza, A.; Chen, P.; Li, Y.; El-Ballat, E.M.; Rauf, A.; Hano, C.; El-Esawi, M.A. HD-ZIP gene family: Potential roles in improving plant growth and regulating stress-responsive mechanisms in plants. *Genes* **2021**, *12*, 1256. [CrossRef]
58. Schrick, K.; Ahmad, B.; Nguyen, H.V. HD-Zip IV transcription factors: Drivers of epidermal cell fate integrate metabolic signals. *Curr. Opin. Plant Biol.* **2023**, *75*, 102417. [CrossRef]
59. Li, Y.; Liu, Z.; Qanmber, G.; Liu, L.; Shi, H.; Guo, Y.; Yu, M.; Hussain, G.; Peng, F.; Zheng, K.; et al. Evolutionary Diversification and Adaptive Evolution Analysis of the Plant HD-Zip IV Subfamily. *Genes* **2025**, *16*, 1348. [CrossRef]
60. Qiu, X.; Wang, G.; Abou-Elwafa, S.F.; Fu, J.; Liu, Z.; Zhang, P.; Xie, X.; Ku, L.; Ma, Y.; Guan, X.; et al. Genome-wide identification of HD-ZIP transcription factors in maize and their regulatory roles in promoting drought tolerance. *Physiol. Mol. Biol. Plants* **2022**, *28*, 425–437. [CrossRef]
61. Zhang, J.; Zhang, X.; Liu, M.; Jin, Y.; Pai, Q.; Wu, X.; Sun, D. Genome-Wide Identification of the HD-ZIP Transcription Factor Family in Maize and Functional Analysis of the Role of ZmHD-ZIP23 in Seed Size. *Plants* **2025**, *14*, 2477. [CrossRef]

Disclaimer/Publisher's Note: The statements, opinions and data contained in all publications are solely those of the individual author(s) and contributor(s) and not of MDPI and/or the editor(s). MDPI and/or the editor(s) disclaim responsibility for any injury to people or property resulting from any ideas, methods, instructions or products referred to in the content.